Author Manuscript

Author Manuscript

Author Manuscript

Author Manuscript

HHS Public Access

Author manuscript

Cell Rep. Author manuscript; available in PMC 2018 August 08.

Published in final edited form as:

Cell Rep. 2017 November 28; 21(9): 2458–2470. doi:10.1016/j.celrep.2017.11.003.

Pancreatic Adenocarcinoma Therapeutic Targets Revealed by Tumor-Stroma Cross-Talk Analyses in Patient-Derived Xenografts

Rémy Nicolle[1,*,10,11], **Yuna Blum**[1,10], **Laetitia Marisa**[1,10], **Celine Loncle**[2], **Odile Gayet**[2], **Vincent Moutardier**[3,4], **Olivier Turrini**[4,5], **Marc Giovannini**[5], **Benjamin Bian**[2], **Martin Bigonnet**[2], **Marion Rubis**[2], **Nabila Elarouci**[1], **Lucile Armenoult**[1], **Mira Ayadi**[1], **Pauline Duconseil**[2], **Mohamed Gasmi**[3], **Mehdi Ouaissi**[5], **Aurélie Maignan**[2], **Gwen Lomberk**[7], **Jean-Marie Boher**[5], **Jacques Ewald**[5], **Erwan Bories**[5], **Jonathan Garnier**[2], **Anthony Goncalves**[4,5], **Flora Poizat**[5], **Jean-Luc Raoul**[4,5], **Veronique Secq**[3], **Stephane Garcia**[3,4], **Philippe Grandval**[4,6], **Marine Barraud-Blanc**[6], **Emmanuelle Norguet**[6], **Marine Gilabert**[5], **Jean-Robert Delpero**[4,5], **Julie Roques**[2], **Ezequiel Calvo**[8], **Fabienne Guillaumond**[2], **Sophie Vasseur**[2], **Raul Urrutia**[9], **Aurélien de Reyniés**[1], **Nelson Dusetti**[2], and **Juan Iovanna**[2,*]

[1]Programme Cartes d'Identité des Tumeurs (CIT), Ligue Nationale Contre le Cancer, Paris, France

[2]Centre de Recherche en Cancérologie de Marseille (CRCM), INSERM U1068, CNRS UMR 7258, Institut Paoli-Calmettes, Aix Marseille Université, Marseille, France

[3]Hôpital Nord, Marseille, France

[4]Aix Marseille Université, Marseille, France

[5]Institut Paoli-Calmettes, Marseille, France

[6]Hôpital de la Timone, Marseille, France

[7]Division of Research, Department of Surgery, Medical College of Wisconsin, Milwaukee, WI 53226, USA

This is an open access article under the CC BY-NC-ND license (http://creativecommons.org/licenses/by-nc-nd/4.0/).

*Correspondence: remy.nicolle@ligue-cancer.net (R.N.), juan.iovanna@inserm.fr (J.I.).
[10]These authors contributed equally
[11]Lead Contact

DATA AND SOFTWARE AVAILABILITY

The accession number for exome sequencing reported in this paper is EMBL-EBI: EGAS00001001928. The accession number for SNP arrays reported in this paper is EMBL-EBI: E-MTAB-5006. The accession number for the ethylation array reported in this paper is EMBL-EBI: E-MTAB-5008. The accession numbers for miRNA-seq and RNA-seq reported in this paper are EMBL-EBI: E-MTAB-5018 and E-MTAB-5039, respectively.

SUPPLEMENTAL INFORMATION

Supplemental Information includes Supplemental Experimental Procedures, six figures, and four tables and can be found with this article online at https://doi.org/10.1016/j.celrep.2017.11.003.

AUTHOR CONTRIBUTIONS

C.L., O.G., B.B., M.B., L.A., M.A., P.D., A.M., and J.G. performed the biological experiments and sample preparation. M.A. and N.E. conducted data management. M.R., V.S., S.G., J.R., and F.P. performed the histochemical stainings and immunohistochemical scoring. V.M., O.T., M. Giovannini, M. Gasmi, M.O., J.E., E.B., A.G., J-L.R., P.G., M.B.-B., E.N., M. Gilabert, F.G., S.V., and J.-R.D. provided material. R.N., Y.B., and L.M. performed bioinformatics analysis. R.N., Y.B., L.M., G.L., J.-M.B., E.C., R.U., A.d.R., N.D., and J.I. contributed to the experimental design, data analysis and discussion. A.d.R., N.D., and J.I. directed the project. R.N., Y.B., L.M., N.D., and J.I. wrote the manuscript.

[8]Centre Génomique du Centre de Recherche du CHUL Research Center, Ville de Québec, QC, Canada

[9]Division of Research, Department of Surgery, Genomic Sciences and Precision Medicine Center, Medical College of Wisconsin, Milwaukee, WI 53226, USA

SUMMARY

Preclinical models based on patient-derived xenografts have remarkable specificity in distinguishing transformed human tumor cells from non-transformed murine stromal cells computationally. We obtained 29 pancreatic ductal adenocarcinoma (PDAC) xenografts from either resectable or non-resectable patients (surgery and endoscopic ultrasound-guided fine-needle aspirate, respectively). Extensive multiomic profiling revealed two subtypes with distinct clinical outcomes. These subtypes uncovered specific alterations in DNA methylation and transcription as well as in signaling pathways involved in tumor-stromal cross-talk. The analysis of these pathways indicates therapeutic opportunities for targeting both compartments and their interactions. In particular, we show that inhibiting NPC1L1 with Ezetimibe, a clinically available drug, might be an efficient approach for treating pancreatic cancers. These findings uncover the complex and diverse interplay between PDAC tumors and the stroma and demonstrate the pivotal role of xenografts for drug discovery and relevance to PDAC.

In Brief

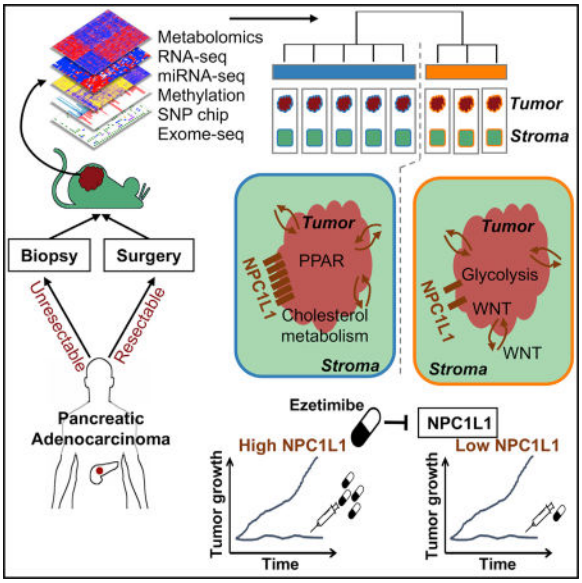

Nicolle et al. present a genomic analysis of pancreatic cancer xenografts showing that tumor subtypes are defined by specific epigenetic, transcriptional, and stromal landscapes. They reveal potential therapeutic targets through analysis of signaling cross-talk between tumor and stromal cells.

Author Manuscript Author Manuscript Author Manuscript Author Manuscript

Author Manuscript Author Manuscript Author Manuscript Author Manuscript

INTRODUCTION

Stratifying tumors using genome-wide molecular profiles has proven to be valuable for predicting therapeutic responses and clinical outcome in many neoplastic diseases. While pancreatic ductal adenocarcinoma (PDAC) is the fourth leading cause of cancer-related deaths, few integrative genomic, epigenomic, and transcriptomic studies have been conducted (Bailey et al., 2016; Cancer Genome Atlas Research Network [TCGA], 2017). This is mainly due to difficulty in obtaining an appropriate series of PDAC tumor samples. A major obstacle is the requirement for surgical samples resulting in the exclusion of the 85% non-resectable patients. Another critical issue is the high proportion of non-transformed stromal cells infiltrating the tumor, which greatly hinders the analysis of carcinogenic-specific processes. Despite these difficulties, the diversity of PDAC has been investigated recently using genome-wide approaches on surgical samples. A canonical study combining elegant laser capture microdissection followed by transcriptomic analysis revealed three main groups of patients: classical, quasi-mesenchymal, and exocrine-like (Collisson et al., 2011). The defined subtypes were suggested to differ in their clinical outcome and therapeutic responses. Another interesting study designed for tumor stratification and drug sensitivity reproduced this classification on a small number of samples (Noll et al., 2016). Moffitt and colleagues (Moffitt et al., 2015) involved a sophisticated computational approach using transcriptomic data and isolated cancerous, stromal, and normal tissue gene expression profiles. Analysis of estimated cancer-specific profiles identified two main tumor subtypes, including a basal-like subtype with a poor clinical outcome that bears great similarity to the basal-like tumors described in bladder and breast cancers. This study suggested that the exocrine-like subtype is attributable to the presence of normal non-transformed pancreatic endocrine/exocrine epithelium. More recently, the Australian pancreatic cancer ICGC (International Cancer Genome Consortium) project defined four subtypes of PDAC based on the transcriptomic analysis of 96 selected primary tumors (Bailey et al., 2016), which they named squamous, pancreatic progenitor, immunogenic, and aberrantly differentiated endocrine exocrine (ADEX). Overall, solely based on gene expression, these studies recurrently found one specific subtype associated with a poor prognosis and a loss of differentiation that was either termed quasi-mesenchymal, basal-like, or squamous. However, no consensus arose from the subdivision of the well-differentiated PDAC tumors, particularly as none of the non-basal subtypes that were proposed are distinguishable based on their clinical outcome. In addition to the lack of non-resectable tumors, only one study proposed a model of the function and diversity of PDAC stroma (Bailey et al., 2016; Moffitt et al., 2015). Indeed, while the extensive desmoplasia present in PDAC tumors has raised major interrogations of its clinical impact and, more generally, on its function in the carcinogenic process (Carapuça et al., 2016; Rhim et al., 2014; Sherman et al., 2014; Tape et al., 2016), large-scale studies of the pancreatic tumor microenvironment are lacking.

Patient-derived xenografts (PDXs) are progressively appearing as a prime approach for much-needed preclinical studies and, in particular, to characterize drug efficacy by simulating phase II clinical trials (Gao et al., 2015; Townsend et al., 2016). PDXs have major advantages over cell lines as models of primary cancers. For instance, tumor cells

Author Manuscript Author Manuscript Author Manuscript Author Manuscript

preserve their complex 3D organization by being embedded in an active microenvironment with an elaborate and dynamic cellular composition. Importantly, xenografts of human primary PDAC enable "*ex patient*," but *in vivo*, studies and through consecutive passages allow characterization of the tumor even after patient mortality. Although there are limitations, particularly related to the host environment, PDX is probably the closest currently available model to the human disease. Several studies in bladder (Pan et al., 2015), colorectal cancer, and lymphoma (Song et al., 2016) have shown the similarities between primary tumors and PDX, with a particular emphasis on genomic alterations. Importantly, a study on PDAC and hepatocellular carcinoma PDX suggested that the main differences in gene expression between primary tumors and xenografts are due to the difficulty of profiling the murine stroma using microarrays (Martinez-Garcia et al., 2014), as they measure human gene expression. With the advent of sequencing-based transcriptomic profiling, PDX offers an ideal setting to distinguish and study the interactions between the tumor and stromal cells. Indeed, sequencing profiles of a mix of human grafted cancerous and infiltrating mouse stromal cells can be analyzed separately *in silico* by unambiguously assigning each sequence to the human or mouse genome (Bradford et al., 2013). However, although PDX models are increasingly used in preclinical studies, they are insufficiently characterized, as few studies have addressed the question of their relevance as a model of the diversity of human disease (Witkiewicz et al., 2016). Finally, we expect that the integrated analysis of PDX multiomics profiles will reveal therapeutic targets for this disease.

RESULTS

PDX Establishment and Validation of the Model

Following suspicion of PDAC, the endoscopic ultrasound-guided fine-needle aspirates of non-resectable tumors or surgical samples of resectable tumors were used to generate subcutaneous xenografts in immunocompromised mice. Histological comparison of resected primary tumors with their correspondent PDX demonstrated extensive similarities (Figure S1A). Early passage of 29 patient-derived xenografts (30 xenograft samples in all) were used to generate genomic, epigenomic, and transcriptomic profiles (Figure 1A). In order to accurately analyze bulk xenograft samples, we developed a methodology that we termed SMAP (simultaneous mapping for patient-derived xenograft), which uses both the human and mouse genomes to distinguish reads from the tumor and stromal compartment, respectively (see Supplemental Information). The separation of species-specific RNA reads resulted in two transcriptomic profiles for each sample: one tumor profile based on human RNA sequences from the grafted tumor cells and one stromal profile from the mouse RNA sequences.

To validate PDX as a model of the primary tumor, the transcriptomes were compared to the virtually microdissected expression signatures that were recently proposed as associated with the tumor or stromal cells of primary human PDAC (Moffitt et al., 2015). The immune signature and the two stromal signatures (normal and activated) were predominantly expressed by the murine stromal cells, while the two cancer signatures (basal-like and classical) were expressed by the human tumor cells (Figures 1B and S1B). This clear distinction of the grafted human tumor cells and the recruited murine stromal cells provides

Author Manuscript Author Manuscript Author Manuscript Author Manuscript

the means to identify potential tumor-stroma interactions from the analysis of a bulk xenograft sample. The combined analysis of both murine and human transcriptomes highlighted several well-described tumor-stroma interactions, such as the activation of MET and insulin growth factor (IGF)1R in tumor cells by the stromal-expressed HGF and IGF, respectively (Figures 1C and S1C; Table S1). Interestingly, 9 out of 17 stromal genes shown in Figure 1C are part of the activated stromal signature previously defined in human primary tumors (Moffitt et al., 2015). Overall, these results illustrate the relevance of the PDX model, in particular, in the establishment of a dialog between the grafted cells and their host microenvironment.

Mirrored Tumor-Stroma Classification

In order to uncover the tumor diversity of PDAC using PDX, unsupervised analyses were carried out independently on each of the tumor-specific genome-wide molecular profiles: protein coding mRNA, long non-coding RNA, microRNA, and non-island and island CpG methylation. The resulting classifications consistently characterized two subtypes defined by the nearly identical sets of samples (Figures 2A and S2A–S2F; Table S2). This marked convergence was summarized in a consensus multiomics classification composed of two subtypes, basal (orange) and classical (blue), as well as two samples with discrepancies between their single-omics classification that will be referred to as outliers (gray) (Figure 2A). Although non-island methylation was consistent with the other single-omics, the island methylation classification revealed a subgroup of CIMP (CpG island methylator phenotype) tumors within the classical subtype (Figure 2B). Virtually, no genes were found to be significantly differentially expressed in association to the CIMP in this cohort (Figures S2G–S2I; Table S2). Moreover, the genes that were associated with the CIMP hypermethylated CpG were more often found to be underexpressed in all classical samples (64 of the 184 hypermethylated genes found significantly underexpressed in classical samples as compared to basal samples) than specifically underexpressed in CIMP samples (neither of the 2 genes were found to be underexpressed in CIMP samples). These results suggest that the CIMP is only one of the mechanism-silencing genes in classical samples, while the others are yet to be discovered.

Global genomic properties such as chromosomal instability index (CIN) or mutation rate showed no specific association with the classification (Figure 2B). Unsurprisingly, genomic alterations that are commonly found in PDAC (*KRAS* mutations, *SMAD4* losses, *CDKN2A* inactivation, *myc* amplification, etc.), were also widespread in PDX (Figure S2J). However, none of these alterations and none of any of the genomic alteration events, including potential gene fusions (Table S2), identified in this work were associated with the basal or classical subtype. As previously observed (Bailey et al., 2016), *TP53* showed a slightly higher mutation rate in the basal subtype, although with virtually no discriminative power. Besides the absence of subtype-specific single alterations, the unsupervised classification of copy number aberrations also showed no association (Figure S2K). This lack of genetic support for the two PDAC subtypes has been suggested in a larger series of patients using whole-genome sequencing (Bailey et al., 2016). However, the remarkable parallel between the transcriptome and methylome suggests that the main phenotypes in PDAC are epigenetically rather than genetically established.

Author Manuscript Author Manuscript Author Manuscript Author Manuscript

Clinical and histopathological characterizations revealed that patients of the basal subtype were more often non-resectable, had a marginally lower median survival, and presented a less differentiated tumor (Figures 2C and S2L), altogether indicating a more aggressive phenotype. Conversely, classical tumors were more frequently resectable, presented a higher level of differentiation, and were often associated with fibrosis and inflammation. In order to compare these PDX-based subtypes with currently available human PDAC classifications, methylome and gene expression classifiers were constructed from three different public datasets (Collisson et al., 2011), (Moffitt et al., 2015), ICGC methylation (Nones et al., 2014) and RNA sequencing (RNA-seq) (Bailey et al., 2016). All published PDAC classification systems were in agreement with the proposed multiomics classification, thereby illustrating the reliability of PDX to model PDAC diversity (Figures 2D and S3A–S3D). Altogether, our analysis on cancer cells using either PDX or human PDAC classifications reveals the presence of two clinically relevant types of PDAC.

Unsupervised analysis of the stromal transcriptomes reconstructed from the murine RNA sequences also revealed two types of stroma with a strong agreement with tumor subtypes (Figure 2E). In order to evaluate this remarkable echo in the diversity of the tumor cells and of their stroma, the tumor and stroma PDAC PDX subtypes were predicted in four public datasets of human primary PDAC. To do so, we derived a tumor and a stromal gene signature predictive of PDAC subtypes based on tumor and stromal expression, respectively. A minor overlap was found between the genes of these signatures, a majority of which encoded cell communication proteins or extra-cellular components (e.g., semaphorins, cytokines; Table S2). The stromal and tumor subtype prediction made by these gene signatures significantly matched in all four primary human tumor datasets, which confirms the mirrored tumor-stromal classification observed in xenografts (Figure S3E).

Interestingly, two recent studies on bulk primary human pancreatic tumors proposed a classification that was suggested to be linked to the stromal composition. The first, by Moffitt et al., described an activated stroma that was linked to a poor outcome (Moffitt et al., 2015) and recently associated with the basal subtype (Bailey et al., 2016). The second was the immunogenic group, which was suggested to be driven by a strong infiltration of immune cells. In order to further characterize the stroma of PDX, a blind source separation algorithm, independent component analysis, was used to extract two components from the stromal transcriptomes (Table S2). The first component was weakly associated with the basal subtype and mostly composed of genes that define the proposed activated stroma of primary PDAC (Moffitt et al., 2015) (Figure S3F). The genes contributing to this component observed in the stroma of xenograft suggest a gradient in stromal activation. Similar to observations in primary human PDAC, the xenografts with a strong activation of their stroma have a marginal tendency to be associated with patients with lower survival (Figure S3G). The second component was strongly associated with the classical subtype as well as with the immunogenic class predictor applied to the stroma (Figure 2F). The immune aspect of this component was supported by its correlation with the infiltration of several populations of immune cells estimated using MCPcounter (Becht et al., 2016) (Figure 2G). Remarkably, these results show that, although the mouse hosts are immunodeprived, PDX tumor models are able to reproduce an immune-related phenotype observed in human primary tumors.

Author Manuscript Author Manuscript Author Manuscript Author Manuscript

Basal Subtype Characterization

The precise sequence-based dissociation of tumor and stroma transcriptomic profiles offers the possibility to rigorously analyze the carcinogenic processes of tumor cells in a subtype-specific approach (Table S3). The basal subtype showed significant deregulations in oncogenic-related pathways and, in particular, a strong overexpression of cell-cycle genes (Figure 3A). The upregulation of the glycolysis in basal tumor cells is in line with a recent description of a group of glycolytic PDAC cell lines associated with a characteristic mesenchymal phenotype (Daemen et al., 2015). Several pathways were also associated with a differential methylated pattern as well as miRNA-based deregulations. This supports the hypothesis that PDAC diversity and the specificities in carcinogenic development of each subtype are epigenetically rather than genetically driven.

In addition to the description of basal tumor cell pathways, the differential analysis of basal stromal pathways was also carried out. The genes involved in focal adhesion and axon guidance pathways, which imply complex interactions with the surrounding tissues, were overexpressed by the tumor and stromal compartments. Along with the enrichment of basal PDX in fibroblasts (Figure 2G), this result suggests a basal-specific communication between tumor cells and adjacent fibroblasts, which is in agreement with recent observations in PDAC of the role of cancer-associated fibroblasts in axon guidance signaling (Secq et al., 2015). In order to validate the transcriptional activation of these pathways in human primary PDAC, an identical pathway analysis was performed on three independent datasets (Figure 3A). The results consistently showed that human basal PDAC activated all of the pathways highlighted in basal PDX. Moreover, the comparison between basal cancer and normal pancreatic transcriptomes showed that these pathway upregulations were cancer specific. Figure 3B schematically illustrates the means by which transcriptional and epigenetic alterations stimulate the highly deregulated WNT pathway. Wnt signaling is potentially activated by tumor cells in an autocrine manner through the upregulation of several WNT ligands, as well as in a paracrine manner by the stromal upregulation of distinct WNT ligands. Finally, the analysis of the methylation patterns suggests a sustained activation of the entire pathway as shown by aberrant methylation of effectors at nearly every step of the signaling cascade as well as of inhibitors of the pathway (Figure S4A).

Classical Subtype Characterization

The analysis of transcriptionally upregulated genes in classical PDX revealed the activation of many pathways (Figure 4A). The upregulation of all of the highlighted pathways was verified in an equivalent differential analysis on human primary PDAC. Importantly, several of these were also found to be active in normal pancreatic samples, suggesting an aberrant differentiated phenotype. Interestingly, a majority of classical-specific pathways relate to either pancreatic digestive function (fat and protein digestion, pancreatic and bile secretion), metabolite transport (fat and protein absorption, small molecule transport), or metabolic pathways (glucose, fructose, mannose, arginine, proline, linoleic, and arachidonic acid metabolism). These results suggest that Classical tumor cells acquire cellular functions usually imputed to other gastrointestinal tissues (*e.g.* enterocytes), in addition to retaining some level of pancreatic digestive function. This is in line with the previous description of the Classical subtype as Progenitor, although we speculate it may acquire some

Author Manuscript Author Manuscript Author Manuscript Author Manuscript

characteristics of a more general gastrointestinal progenitor. Unlike the previously proposed exocrine-like or ADEX PDAC subtypes, we observe here that the Classical subtype maintains a lower level of a more general digestive activity, including product breakdown and uptake that could be used to fuel high metabolic needs. Altogether, we describe the Classical subtype as closer to normal pancreatic tissue than the Basal subtype yet, we do not identify any acinar-like or any differentiated pancreatic subtypes which would only harbor functions and markers of the exocrine or endocrine pancreas.

In order to further characterize the molecular phenotypes of these PDXs, extensive metabolomics profiles, including lipidomics, were generated. Differential analysis of metabolite quantifications supported this hypothesis by demonstrating a general increase in REDOX-related metabolites (Figure S4B; Table S4), previously associated with well-differentiated PDAC cell lines (Daemen et al., 2015). The potential digestive activity was particularly demonstrated by the decline in triacylglicerols associated with an increased lipase expression and an increased level of fatty acids (Figure 4B). In addition, classical tumors also displayed an increase in several glycerophospholipids (Figure S4C), altogether indicating a broad deregulation of the lipid metabolism, as suggested in a previous metabolomics study on PDAC cell lines (Daemen et al., 2015).

Figure 5 shows a partial view of the range of small molecule transporters overexpressed in classical samples, which include the upregulation of the glucose (*SLC2A2*) and glutamine (*SLC1A1*) transporters, which are strongly hypomethylated in classical samples (Figure S4D). Glutamine is a necessary nitrogen donor for the initial steps of nucleotide biosynthesis. Interestingly, the upregulation and epigenetic deregulation of the glutamine transporter in classical tumors is associated to a strong increase in two nucleotides, inosine monophosphate (IMP) and uridine monophosphate (UMP) (Figure S4E). Cholesterol transporters were also significantly upregulated; in particular, the overexpression of the intestinal cholesterol uptake regulator *NPC1L1* was associated to extensive hypomethylation (Figure 5). Aberrant cholesterol uptake has been recently implicated in the proliferation and survival of pancreatic cancer cells (Guillaumond et al., 2015). Metabolomics profiling revealed a significantly higher level of cholesteryl ester in classical PDX (Figure 5), supporting an increased absorption activity. Moreover, the analysis of the stroma of classical tumors highlighted the upregulation of genes involved in lipid metabolism and cholesterol synthesis, as well as the master regulators of lipid and cholesterol homeostasis, namely, *PPARG* and *NR1H3* (LXRα). Altogether, these results suggest an active cross-talk involving the stromal synthesis of cholesterol associated with aberrant nutrient uptake by classical tumor cells.

In order to validate the predicted compartment-specific expression of genes of interest, immunohistochemical staining was performed. As a control, *MUC17*, which was expressed by classical tumor cells displayed no protein expression in basal tumors, as expected (Figures S5A and S5B). Immunohistochemical staining of PPARG and its target FABP5 confirmed transcriptomic data by validating their expression in classical stromal cells (Figures S5C and S5D).

Author Manuscript Author Manuscript Author Manuscript Author Manuscript

Evidence of Potential Therapeutic Targets

Despite the absence of any specific druggable genetic alterations, the integrative multiomics analysis uncovered epigenetically deregulated pathways in PDAC subtypes with high potential druggability (e.g., WNT, *EGFR, PPARG*, small molecule transporters). In particular, our integrated analysis examined the stroma as well as the epigenetic deregulation of cholesterol metabolism and uptake. Moreover, cholesterol metabolism was recently associated with pancreatic cancer in cellular and epidemiological studies (Chen et al., 2015; Guillaumond et al., 2015). As a proof of concept for defining therapeutic targets from the integrated multiomics analysis of PDX, we selected the highly epigenetically deregulated *NPC1L1*, for which an efficient inhibitor is clinically available: Ezetimibe. DNA demethylation using 5-Aza-2′-deoxycytidine confirmed the epigenetic regulation of *NPC1L1* (Figure S6A). Immunohistochemical staining confirmed the protein expression of *NPC1L1* and its correlation with mRNA levels, overall showing higher levels in classical tumors (Figures 6A and S6B).

Sensitivity analysis of Ezetimibe on the survival of 4 basal and 3 classical PDX-derived cell cultures expressing different levels of *NPC1L1* revealed that all PDAC cells are sensitive to the inhibitor, while the treatment had little to no effect on fibroblasts (Figures 6B and S6C). However, as Ezetimibe functions as a competitor of cholesterol, cells expressing lower levels of *NPC1L1* (i.e., Basal) were highly sensitive, while cells with high levels of *NPC1L1* (i.e., Classical) required greater inhibitor quantities (Figure 6C). This result suggests that *NPC1L1* and, by extension, the cholesterol metabolism have a major role in both Basal and Classical PDAC. In addition, the combination of gemcitabine with Ezetimibe did not affect the cytotoxic effect of gemcitabine in PDAC cells (Figure S6D).

In order to study the specificity of *NPC1L1* inhibition on PDAC survival, targeted small interfering RNA (siRNA) knockdown was performed. This genetic approach revealed a dramatic effect on the survival of the siRNA-transfected cells validating the role of *NPC1L1* as an original therapeutic target (Figure 6D). The knockdown of *NPC1L1* made cells resistant to high levels of Ezetimibe, providing evidence for the specificity of the treatment (Figures S6E and S6F). We then derived spheroids and organoids from PDX and treated these structures with Ezetimibe for 3 and 4 days, respectively, as shown in Figures 6E and 6G. Ezetimibe treatment resulted in a significant effect on their growth, as measured by cell viability (Figures 6F and 6I) and volume change (Figure 6H). Finally, we performed a preclinical analysis by treating two PDXs with Ezetimibe (5 mg/day) in 200 mL corn oil by a daily intraperitoneal (i.p.) injection to confirm the *in vitro* results. As shown in Figure 6J, PDAC019T (classical) and PDAC003T (basal) samples efficiently responded to the treatment by reducing their growth. Based on these *in vitro* and *in vivo* results, we conclude that *NPC1L1* is a highly effective therapeutic target for treating PDAC using Ezetimibe.

DISCUSSION

We report in this work the use of PDXs to profile both resectable as well as non-resectable PDAC. We found that PDXs obtained by biopsied PDAC are frequently associated with a more aggressive phenotype, suggesting that studies profiling PDAC still present a bias. Moreover, one advantage of a xenograft is to combine transformed tumor and stromal cells

Author Manuscript Author Manuscript Author Manuscript Author Manuscript

from distinct species, resulting in the ability to investigate cancer and stromal molecular profiles independently. Analysis of tumor-cell-specific molecular profiles allowed the examination of epigenetic and transcriptomic profiles, separately from non-neoplastic signals. Conversely, the absence of relationship between the consensus multiomics classification and genomic alterations, which was previously proposed, is unambiguously confirmed in this work. This is a crucial confirmation, since it supports the idea of an epigenetic identity for PDAC subtypes. The most likely explanation for this observation is that genetic mutations, amplifications, and deletions are involved in the transformation process of PDAC, whereas the clinical outcome, response to treatments, and the phenotype of the tumors are controlled at the epigenetic level. This observation is of obvious clinical relevance, since emerging epigenetic drugs can be used to target these tumor characteristics and, therefore, opens a promising avenue in the treatment of PDAC patients. While preliminary genomic analysis suggested that genetic alteration could define therapeutic options (Witkiewicz et al., 2015), more recent studies found no associations between any genetic alterations and therapeutic responses on a large number of drugs (Knudsen et al., 2017; Witkiewicz et al., 2016).

Based on the analysis of PDX, we identified two major subtypes with extensive similarities to the basal and classical human PDAC subtypes. The specific analysis of the tumor cell profiles underlined the homogeneity of basal samples while highlighting the diversity of the classical subtype. For instance, while CIMP PDACs have been described (Ueki et al., 2000), we found that this phenotype corresponds to a subdivision of classical PDAC exclusively. Overall, the two molecular subtypes describe two distinct PDAC development patterns: a dedifferentiated basal subtype, highly glycolytic and with features associated with epithelial-mesenchymal transition, and a subtype with more general digestive differentiation features reminiscent of an aberrant gastro-intestinal progenitor. In addition to having distinct and specific signaling exchanges with their stroma, a broad homogeneity among all samples can be observed in some major tumorstroma pathways (e.g., HGF, IGF, and Hedgehog). Despite the PDX being hosted in immunodeprived mice, we found a subgroup of samples in the classical PDX group with extensive immune infiltration that strongly correlated with the immunogenic subtype described in primary PDAC (Bailey et al., 2016). Our observations indicate that this subgroup is broadly driven by its stromal content and is, in fact, a “classical inflammatory infiltrated” subtype instead of a specific subtype by itself. Although these models are not suitable to study immune therapy, these results show the extent to which xenografts can reproduce primary PDAC phenotypes, including interaction with the immune microenvironment. Importantly, athymic NMRI nude mice (*Foxn1nu*) lack conventional T cell development, but this does not preclude extrathymic maturation such as intestinal T cell differentiation, which likely explains the extensive infiltration of the immunogenic-like PDX. Although nude mice lack thymus-dependent lymphocytes, other immune cell populations such as macrophages, natural killers and B cells are present and functional. Given the potential of PDX to reproduce an immunogenic PDAC subtype in a model with an only partial immune landscape, new developments in animal models, in particular humanized mice, can be expected to greatly improve the present model and potentially be used to investigate immune therapies.

Author Manuscript Author Manuscript Author Manuscript Author Manuscript

In addition to greatly improving the multiomics description of tumor-specific altered pathways, the precise distinction of tumor and stromal cells in the same samples enabled analysis of crosstalk at the genome-wide level. The simple description of the most expressed genes in each compartment highlighted known molecular dialogs between tumor cells and their stroma. The role of PDAC stroma on tumor survival and growth is not settled. It was previously suggested that the stroma plays a major role in the resistance to the PDAC treatments, because it acts as a mechanical barrier impeding the access of the drugs and also inhibits the formation of vessels. Therefore, it seemed important to combine agents against cancer cells with compounds targeting the stroma to improve efficiency. Accordingly, recent results encourage going forward in this way. In fact, initial testing of the Hedgehog signaling pathway inhibitor IPI-926 demonstrated a promising transient effect on the tumor microenvironment, leading to improved drug delivery and an association with improved survival in mice treated with both IPI-926 and gemcitabine (Olive et al., 2009). Mouse models of PDAC deficient in Sonic Hedgehog (Rhim et al., 2014) demonstrated that Hedgehog inhibition leads to an absence of tumor stroma and an abundance of intratumoral blood vessels yet increases tumor aggressiveness and metastasis. Another potential stroma-targeting therapy relates to glycosaminoglycan hyaluronan, which is overrepresented in PDAC stroma and which can be degraded by hyaluronidase. Notably, treatment with PEGPH20, a PEGylated human recombinant hyaluronidase, induces a rapid perfusion increase, leading to the inhibition of growth when combined with chemotherapy in mouse PDAC models (Walker et al., 2015). While the outcome of stroma-targeting therapies remains unknown, major signaling pathways driving PDAC have been shown to be stimulated by the non-transformed cells composing its microenvironment. Our work revealed the potential sustaining role of the stroma as subtype specific. Indeed, the analysis of the recruited stroma diversity revealed the unidentified subtype specificity of the stroma through the discovery of convergent tumor/stromal classifications, which was verified in four different datasets of primary tumors. This is, to some extent, dissimilar to the activated stroma previously described (Moffitt et al., 2015) as subtype independent. Overall, our results show that the stroma, originating from surrounding host cells, is closely associated with the phenotype of the tumor indicating that the composition and function of the tumor microenvironment may be trained by tumor cells.

A major advantage of the PDX model is that it is a perpetual source of living material conserving original biological characteristics. Indeed, each PDX can be molecularly analyzed and concomitantly used for testing biological hypotheses or putative therapeutic targets derived from these analyses. In this work, we describe several subtype-specific pathways, thereby highlighting potential targeted therapies. We used *NPC1L1*, a transporter of cholesterol, as a proof of concept of an original candidate to be targeted for treating PDAC. The function of this gene can be inhibited by a specific inhibitor, Ezetimibe, which has been routinely used for the treatment of hypercholesterolemia. While no studies describe the association of *NPC1L1* or its inhibitor with pancreatic cancer, statins (used for the treatment of hypercholesterolemia) were shown in epidemiological studies to reduce the risks of pancreatic cancer (Walker et al., 2015) and to improve survival (Huang et al., 2016; Wu et al., 2015). Preclinical tests demonstrated that using the specific inhibitor Ezetimibe or genetic knockdown approaches results in a dramatic effect on the survival capacity of PDAC

Author Manuscript Author Manuscript Author Manuscript Author Manuscript

cells and on the growth of spheroids and organoids *in vitro* and of PDX *in vivo*. Finally, we also demonstrated that Ezetimibe treatment does not affect the cytotoxicity of gemcitabine, suggesting that patients could be treated with an inhibitor of the *NPC1L1* transporter incombination with a conventional anticancer drug without influencing its effect. Altogether, our data demonstrate that *NPC1L1* is an interesting and promising therapeutic target.

In conclusion, the data presented in this work reveal that PDX is a suitable model for preclinical studies, representing the diversity of the primary cancers in which the stroma is reconstituted. Its multiomics analysis is a rich source of novel and reliable therapeutic targets for treating patients with PDAC.

EXPERIMENTAL PROCEDURES

PDXs

Three expert clinical centers collaborated on this project after receiving ethics review board approval. Patients were included in this project under the Paoli-Calmettes Institute clinical trial number 2011-A01439-32. Consent forms of informed patients were collected and registered in a central database. The tumor tissues used for xenograft generation were deemed excess to that required for the patient's diagnosis. PDAC tissue from surgical samples was fragmented, mixed with 100 μL Matrigel, and implanted with a trocar (10G; Innovative Research of America, Sarasota, FL) in the subcutaneous right upper flank of an anesthetized and disinfected male NMRI-nude mouse. Samples obtained from endoscopic ultrasound-guided fine needle aspiration (EUSFNA) were mixed with 100 μL of Matrigel (BD Biosciences, Franklin Lakes, NJ) and injected in the upper right flank of a male nude mouse (Swiss Nude Mouse Crl:NU(lco)-Foxn1nu; Charles River Laboratories, Wilmington, MA) for the first implantation. When xenografts reached 1 cm^3, these were removed and passed to NMRI-nude mice in the same manner as surgical samples. In total, 30 xenografts from 29 different patients were generated, and early passages were used for large-scale molecular profiling.

Genome-wide Profiles and Data Availability

Genotype data from whole-exome sequencing have been deposited at the European Genome-phenome Archive (EGA; http://www.ebi.ac.uk/ega/), which is hosted by the EBI, under accession number EMBL-EBI: EGAS00001001928. Other datasets are available on ArrayExpress (http://www.ebi.ac.uk/arrayexpress): SNP data are available under accession number EMBL-EBI: E-MTAB-5006, Methylation data are available under accession number EMBL-EBI: E-MTAB-5008, miRNA sequencing data are available under accession number EMBL-EBI: E-MTAB-5018, and mRNA sequencing data are available under accession number EMBL-EBI: E-MTAB-5039. Sequencing datasets were processed using SMAP (see Supplemental Experimental Procedures) to separate mouse and human reads. In addition to raw data, all processed data produced by and used in this study are available through our institutional web portal (http://cit.ligue-cancer.net/pacaomicsdata-web-page), and simple gene-level queries for expression and methylation are available using a custom application (http://cit-apps.ligue-cancer.net/pdac.pacaomics).

Author Manuscript Author Manuscript Author Manuscript Author Manuscript

Public Dataset Comparison

ICGC methylation chips, RNA-seq, and microarray gene expression datasets were downloaded from the ICGC data portal (dcc.icgc.org, release 20). TCGA data were downloaded through the Broad Institute TCGA Genome Data Analysis Center (GDAC) firehose tool (gdac.broadinstitute.org, 20160411 data snapshot). Other datasets were downloaded from the provided GEO entries GSE71729 (Barr et al., 2012, 2010; Moffitt et al., 2015) and GSE17891 (Collisson et al., 2011; Martínez-Arranz et al., 2015; Nones et al., 2014). All non-cancer samples were removed from each dataset. Expression datasets were then centered gene-wise. Centroid classifiers were built for each dataset defining a classification using a Pearson-based approach described in previous work (Bailey et al., 2016; Guinney et al., 2015; Marisa et al., 2013)

Primary Cell Cultures and Sensitivity

Primary cell cultures were obtained from PDX. Ezetimibe was obtained from Selleckchem (ref. S1655). Tissues were split into several small pieces and processed in a biosafety chamber. Five thousand cells per well were plated in 96-well plates in serum-free defined media (SFDM) medium. The RNA profile of each cell culture showed a contamination in murine cells of less than 3%. Twenty-four hours later, the media were supplemented with increasing concentrations of Ezetimibe and incubated for an additional 72-hr period. Cell viability was estimated with the PrestoBlue (Invitrogen, Grand Island, NY) reagent. Each experiment was done in triplicate and repeated at least three times. Six increasing concentrations of Ezetimibe were used ranging from 0 μM to 100 μM.

Spheroid Sensitivity to Ezetimibe

Fifteen thousand cells per well were seeded in 96-well round-bottom plates with medium containing 20% methylcellulose (Sigma-Aldrich, St. Louis, MO, USA). After 48-hr incubation, cells with spheroids of uniform size and shape were incubated with 50 μM Ezetimibe during 72 hr. Spheroid growth was monitored for 96 hr by taking microphotographs every day or assessed with the CellTiter-Glo 3D kit at the end of the treatment according to the manufacturer's instructions (Promega, Madison, WI). Values were normalized and expressed as the percentage of the control treatment (DMSO, 0.05%).

Pancreatic Organoid Generation and Treatment with Ezetimibe

Organoid suspensions obtained from fresh tissue samples were placed into a 12-well plate coated with 100 μL GFR Matrigel. Media were replaced every 2–3 days. Twenty-four hours after seeding, organoids were incubated with 100 μL pancreatic organoid feeding media (POFM) supplemented with 50 μM Ezetimibe or 100 μL POFM supplemented with vehicle (0.5% DMSO) into 96-well plates coated with 15 μL Matrigel GFR. Organoid growth was monitored for 96 hr by taking microphotographs every day or assessed with the CellTiter-Glo 3D kit at the end of the treatment. Values were normalized and expressed as the percentage of the control.

Author Manuscript Author Manuscript Author Manuscript Author Manuscript

Treatment with Ezetimibe of PDX *In Vivo*

We transplanted two PDX samples (PDAC019T and PDAC003T) subcutaneously into 6-week-old male Swiss nude mice (Crl: Nu(lco)-Foxn1nu; Charles River Laboratories, Wilmington, MA). Each PDX sample was inoculated into six nude NMRI mice that were randomized for treatment (n = 3) and vehicle (n = 3). When the PDX reached 100 mm^3, we started the treatment with Ezetimibe or vehicle and followed their growth for 17 days. Ezetimibe was prepared as a solution of 250 mg/mL in ethanol and then resuspended in corn oil at 25 mg/mL, and 200 μL was administered in i.p. injections every day. Tumor size was measured with a Vernier caliper twice weekly, and the tumor volume was calculated with the equation $v = (\text{length}/\text{width}^2)/2$.

Supplementary Material

Refer to Web version on PubMed Central for supplementary material.

Acknowledgments

This work is part of the national program Cartes d'Identité des Tumeurs (CIT) funded and developed by the Ligue Nationale Contre le Cancer. This work was supported by INCa, Canceropôle PACA, Inserm and by DGOS through a SIRIC grant INCa-Inserm-DGOS 1068.

We thank Emilie Nouguerede, Jihane Pakradouni, Karim Sari, and Regis Vitestelle for their technical assistance and Aurélie Kamoun for fruitful discussions.

References

Bailey P, Chang DK, Nones K, Johns AL, Patch A-M, Gingras M-C, Miller DK, Christ AN, Bruxner TJC, Quinn MC, et al. Australian Pancreatic Cancer Genome Initiative. Genomic analyses identify molecular subtypes of pancreatic cancer. Nature. 2016; 531:47–52. [PubMed: 26909576]

Barr J, Vázquez-Chantada M, Alonso C, Pérez-Cormenzana M, Mayo R, Galán A, Caballería J, Martín-Duce A, Tran A, Wagner C, et al. Liquid chromatography-mass spectrometry-based parallel metabolic profiling of human and mouse model serum reveals putative biomarkers associated with the progression of nonalcoholic fatty liver disease. J. Proteome Res. 2010; 9:4501–4512. [PubMed: 20684516]

Barr J, Caballería J, Martínez-Arranz I, Domínguez-Díez A, Alonso C, Muntané J, Pérez-Cormenzana M, García-Monzón C, Mayo R, Martín-Duce A, et al. Obesity-dependent metabolic signatures associated with nonalcoholic fatty liver disease progression. J. Proteome Res. 2012; 11:2521–2532. [PubMed: 22364559]

Becht E, Giraldo NA, Lacroix L, Buttard B, Elarouci N, Petitprez F, Selves J, Laurent-Puig P, Sautès-Fridman C, Fridman WH, de Reyniès A. Estimating the population abundance of tissue-infiltrating immune and stromal cell populations using gene expression. Genome Biol. 2016; 17:218. [PubMed: 27765066]

Bergmann U, Funatomi H, Yokoyama M, Beger HG, Korc M. Insulin-like growth factor I overexpression in human pancreatic cancer: evidence for autocrine and paracrine roles. Cancer Res. 1995; 55:2007–2011. [PubMed: 7743492]

Bradford JR, Farren M, Powell SJ, Runswick S, Weston SL, Brown H, Delpuech O, Wappett M, Smith NR, Carr TH, et al. RNA-seq differentiates tumour and host mRNA expression changes induced by treatment of human tumour xenografts with the VEGFR tyrosine kinase inhibitor cediranib. PLoS ONE. 2013; 8:e66003. [PubMed: 23840389]

Cancer Genome Atlas Research Network. Integrated genomic characterization of pancreatic ductal adenocarcinoma. Cancer Cell. 2017; 32:185–203.e13. [PubMed: 28810144]

Author Manuscript Author Manuscript Author Manuscript Author Manuscript

Carapuça EF, Gemenetzidis E, Feig C, Bapiro TE, Williams MD, Wilson AS, Delvecchio FR, Arumugam P, Grose RP, Lemoine NR, et al. Anti-stromal treatment together with chemotherapy targets multiple signalling pathways in pancreatic adenocarcinoma. J. Pathol. 2016; 239:286–296. [PubMed: 27061193]

Chen H, Qin S, Wang M, Zhang T, Zhang S. Association between cholesterol intake and pancreatic cancer risk: evidence from a meta-analysis. Sci. Rep. 2015; 5:8243. [PubMed: 25649888]

Collisson EA, Sadanandam A, Olson P, Gibb WJ, Truitt M, Gu S, Cooc J, Weinkle J, Kim GE, Jakkula L, et al. Subtypes of pancreatic ductal adenocarcinoma and their differing responses to therapy. Nat. Med. 2011; 17:500–503. [PubMed: 21460848]

Daemen A, Peterson D, Sahu N, McCord R, Du X, Liu B, Kowanetz K, Hong R, Moffat J, Gao M, et al. Metabolite profiling stratifies pancreatic ductal adenocarcinomas into subtypes with distinct sensitivities to metabolic inhibitors. Proc. Natl. Acad. Sci. USA. 2015; 112:E4410–E4417. [PubMed: 26216984]

Farrow B, Berger DH, Rowley D. Tumor-derived pancreatic stellate cells promote pancreatic cancer cell invasion through release of thrombospondin-2. J. Surg. Res. 2009; 156:155–160. [PubMed: 19592030]

Gao H, Korn JM, Ferretti S, Monahan JE, Wang Y, Singh M, Zhang C, Schnell C, Yang G, Zhang Y, et al. High-throughput screening using patient-derived tumor xenografts to predict clinical trial drug response. Nat. Med. 2015; 21:1318–1325. [PubMed: 26479923]

Guillaumond F, Bidaut G, Ouaissi M, Servais S, Gouirand V, Olivares O, Lac S, Borge L, Roques J, Gayet O, et al. Cholesterol uptake disruption, in association with chemotherapy, is a promising combined metabolic therapy for pancreatic adenocarcinoma. Proc. Natl. Acad. Sci. USA. 2015; 112:2473–2478. [PubMed: 25675507]

Guinney J, Dienstmann R, Wang X, de Reyniès A, Schlicker A, Soneson C, Marisa L, Roepman P, Nyamundanda G, Angelino P, et al. The consensus molecular subtypes of colorectal cancer. Nat. Med. 2015; 21:1350–1356. [PubMed: 26457759]

Huang BZ, Chang JI, Li E, Xiang AH, Wu BU. Influence of statins and cholesterol on mortality among patients with pancreatic cancer. J. Natl. Cancer Inst. 2016; 109:djw275.

Knudsen ES, Balaji U, Mannakee B, Vail P, Eslinger C, Moxom C, Mansour J, Witkiewicz AK. Pancreatic cancer cell lines as patient-derived avatars: genetic characterisation and functional utility. Gut. 2017. Published January 10, 2017.

Lonardo E, Hermann PC, Mueller M-T, Huber S, Balic A, Miranda-Lorenzo I, Zagorac S, Alcala S, Rodriguez-Arabaolaza I, Ramirez JC, et al. Nodal/Activin signaling drives self-renewal and tumorigenicity of pancreatic cancer stem cells and provides a target for combined drug therapy. Cell Stem Cell. 2011; 9:433–446. [PubMed: 22056140]

Marisa L, de Reyniès A, Duval A, Selves J, Gaub MP, Vescovo L, Etienne-Grimaldi M-C, Schiappa R, Guenot D, Ayadi M, et al. Gene expression classification of colon cancer into molecular subtypes: characterization, validation, and prognostic value. PLoS Med. 2013; 10:e1001453. [PubMed: 23700391]

Martínez-Arranz I, Mayo R, Pérez-Cormenzana M, Mincholé I, Salazar L, Alonso C, Mato JM. Enhancing metabolomics research through data mining. J. Proteomics. 2015; 127(Pt B):275–288. [PubMed: 25668325]

Martinez-Garcia R, Juan D, Rausell A, Muñoz M, Baños N, Menéndez C, Lopez-Casas PP, Rico D, Valencia A, Hidalgo M. Transcriptional dissection of pancreatic tumors engrafted in mice. Genome Med. 2014; 6:27. [PubMed: 24739241]

Moffitt RA, Marayati R, Flate EL, Volmar KE, Loeza SGH, Hoadley KA, Rashid NU, Williams LA, Eaton SC, Chung AH, et al. Virtual microdissection identifies distinct tumor- and stroma-specific subtypes of pancreatic ductal adenocarcinoma. Nat. Genet. 2015; 47:1168–1178. [PubMed: 26343385]

Noll EM, Eisen C, Stenzinger A, Espinet E, Muckenhuber A, Klein C, Vogel V, Klaus B, Nadler W, Rösli C, et al. CYP3A5 mediates basal and acquired therapy resistance in different subtypes of pancreatic ductal adenocarcinoma. Nat. Med. 2016; 22:278–287. [PubMed: 26855150]

Nones K, Waddell N, Song S, Patch A-M, Miller D, Johns A, Wu J, Kassahn KS, Wood D, Bailey P, et al. APGI. Genome-wide DNA methylation patterns in pancreatic ductal adenocarcinoma reveal

Author Manuscript Author Manuscript Author Manuscript Author Manuscript

epigenetic deregulation of SLIT-ROBO, ITGA2 and MET signaling. Int. J. Cancer. 2014; 135:1110–1118. [PubMed: 24500968]

Ohnishi N, Miyata T, Ohnishi H, Yasuda H, Tamada K, Ueda N, Mashima H, Sugano K. Activin A is an autocrine activator of rat pancreatic stellate cells: potential therapeutic role of follistatin for pancreatic fibrosis. Gut. 2003; 52:1487–1493. [PubMed: 12970143]

Olive KP, Jacobetz MA, Davidson CJ, Gopinathan A, McIntyre D, Honess D, Madhu B, Goldgraben MA, Caldwell ME, Allard D, et al. Inhibition of Hedgehog signaling enhances delivery of chemotherapy in a mouse model of pancreatic cancer. Science. 2009; 324:1457–1461. [PubMed: 19460966]

Pan C-X, Zhang H, Tepper CG, Lin T-Y, Davis RR, Keck J, Ghosh PM, Gill P, Airhart S, Bult C, et al. Development and characterization of bladder cancer patient-derived xenografts for molecularly guided targeted therapy. PLoS ONE. 2015; 10:e0134346. [PubMed: 26270481]

Qian L-W, Mizumoto K, Maehara N, Ohuchida K, Inadome N, Saimura M, Nagai E, Matsumoto K, Nakamura T, Tanaka M. Co-cultivation of pancreatic cancer cells with orthotopic tumor-derived fibroblasts: fibroblasts stimulate tumor cell invasion via HGF secretion whereas cancer cells exert a minor regulative effect on fibroblasts HGF production. Cancer Lett. 2003; 190:105–112. [PubMed: 12536083]

Rhim AD, Oberstein PE, Thomas DH, Mirek ET, Palermo CF, Sastra SA, Dekleva EN, Saunders T, Becerra CP, Tattersall IW, et al. Stromal elements act to restrain, rather than support, pancreatic ductal adenocarcinoma. Cancer Cell. 2014; 25:735–747. [PubMed: 24856585]

Secq V, Leca J, Bressy C, Guillaumond F, Skrobuk P, Nigri J, Lac S, Lavaut M-N, Bui T-T, Thakur AK, et al. Stromal SLIT2 impacts on pancreatic cancer-associated neural remodeling. Cell Death Dis. 2015; 6:e1592. [PubMed: 25590802]

Sherman MH, Yu RT, Engle DD, Ding N, Atkins AR, Tiriac H, Collisson EA, Connor F, Van Dyke T, Kozlov S, et al. Vitamin D receptor-mediated stromal reprogramming suppresses pancreatitis and enhances pancreatic cancer therapy. Cell. 2014; 159:80–93. [PubMed: 25259922]

Song H-N, Lee C, Kim ST, Kim SY, Kim NKD, Jang J, Kang M, Jang H, Ahn S, Kim SH, et al. Molecular characterization of colorectal cancer patients and concomitant patient-derived tumor cell establishment. Oncotarget. 2016; 7:19610–19619. [PubMed: 26909603]

Tape CJ, Ling S, Dimitriadi M, McMahon KM, Worboys JD, Leong HS, Norrie IC, Miller CJ, Poulogiannis G, Lauffenburger DA, Jørgensen C. Oncogenic KRAS regulates tumor cell signaling via stromal reciprocation. Cell. 2016; 165:910–920. [PubMed: 27087446]

Tian H, Callahan CA, DuPree KJ, Darbonne WC, Ahn CP, Scales SJ, de Sauvage FJ. Hedgehog signaling is restricted to the stromal compartment during pancreatic carcinogenesis. Proc. Natl. Acad. Sci. USA. 2009; 106:4254–4259. [PubMed: 19246386]

Topalovski M, Brekken RA. Matrix control of pancreatic cancer: new insights into fibronectin signaling. Cancer Lett. 2016; 381:252–258. [PubMed: 26742464]

Townsend EC, Murakami MA, Christodoulou A, Christie AL, Köster J, DeSouza TA, Morgan EA, Kallgren SP, Liu H, Wu S-C, et al. The public repository of xenografts enables discovery and randomized phase II-like trials in mice. Cancer Cell. 2016; 29:574–586. [PubMed: 27070704]

Ueki T, Toyota M, Sohn T, Yeo CJ, Issa JP, Hruban RH, Goggins M. Hypermethylation of multiple genes in pancreatic adenocarcinoma. Cancer Res. 2000; 60:1835–1839. [PubMed: 10766168]

Walker EJ, Ko AH, Holly EA, Bracci PM. Statin use and risk of pancreatic cancer: results from a large, clinic-based case-control study. Cancer. 2015; 121:1287–1294. [PubMed: 25649483]

Whatcott C, Han H, Posner RG, Von Hoff DD. Tumor-stromal interactions in pancreatic cancer. Crit. Rev. Oncog. 2013; 18:135–151. [PubMed: 23237556]

Witkiewicz AK, McMillan EA, Balaji U, Baek G, Lin W-C, Mansour J, Mollaee M, Wagner K-U, Koduru P, Yopp A, et al. Whole-exome sequencing of pancreatic cancer defines genetic diversity and therapeutic targets. Nat. Commun. 2015; 6:6744. [PubMed: 25855536]

Witkiewicz AK, Balaji U, Eslinger C, McMillan E, Conway W, Posner B, Mills GB, O'Reilly EM, Knudsen ES. Integrated patient-derived models delineate individualized therapeutic vulnerabilities of pancreatic cancer. Cell Rep. 2016; 16:2017–2031. [PubMed: 27498862]

Author Manuscript Author Manuscript Author Manuscript Author Manuscript

Wu BU, Chang J, Jeon CY, Pandol SJ, Huang B, Ngor EW, Difronzo AL, Cooper RM. Impact of statin use on survival in patients undergoing resection for early-stage pancreatic cancer. Am. J. Gastroenterol. 2015; 110:1233–1239. [PubMed: 26195180]

Author Manuscript Author Manuscript Author Manuscript Author Manuscript

Highlights

- Patient xenografts are relevant models of pancreatic cancers and of their stroma
- Xenografts allow the genomic analysis of unresectable pancreatic cancers
- The epigenome, transcriptome, and stroma of pancreatic cancer define two subtypes
- Pancreatic cancer is sensitive to inhibition of NPC1L1 by Ezetimibe

Author Manuscript Author Manuscript Author Manuscript Author Manuscript

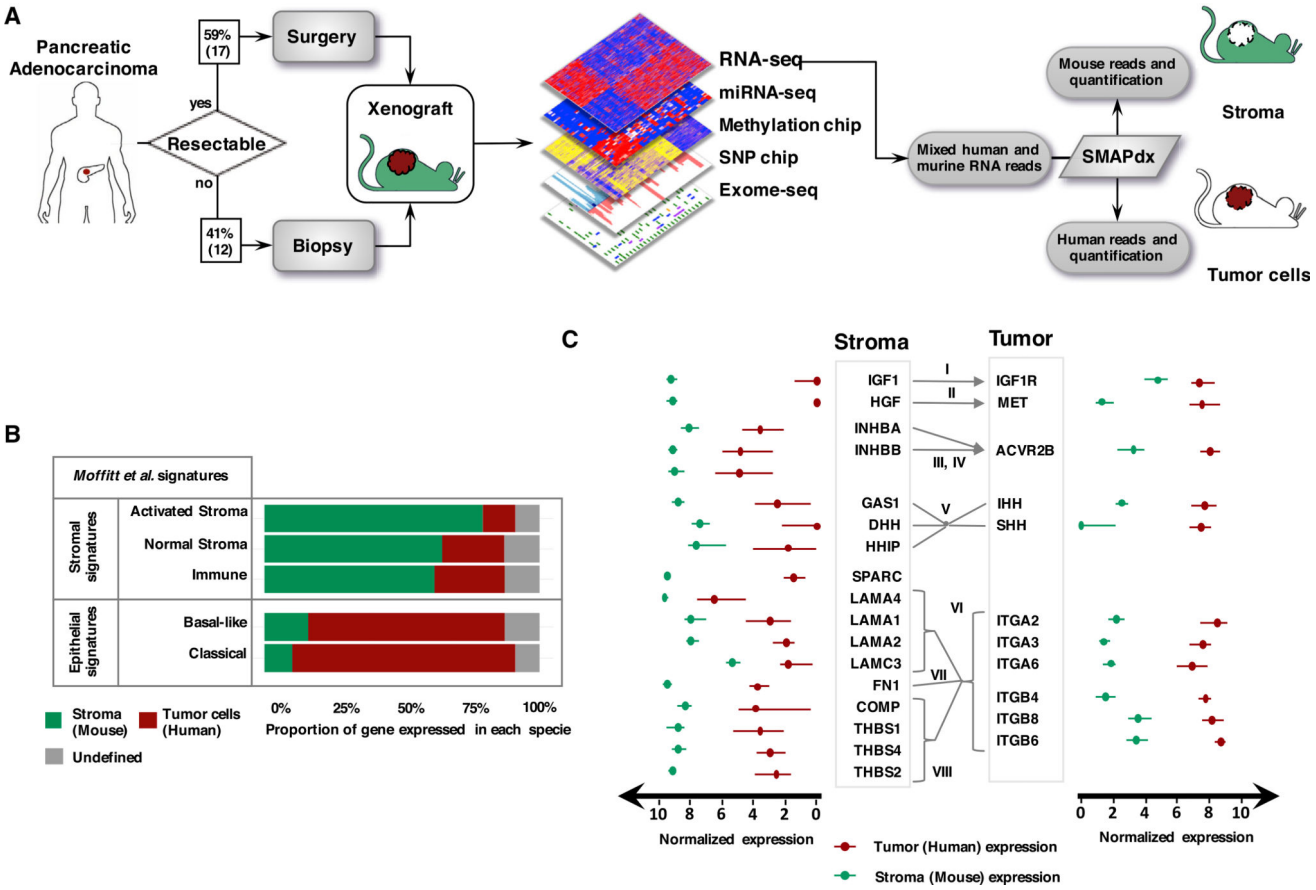

Figure 1. Patient-Derived Pancreatic Adenocarcinoma Xenograft Generation and Characterization

(A) Experimental design for systematic PDX generation followed by molecular tumor and stromal cell characterization. Numbers of biopsy and surgical samples are indicated.

(B) Expression of human primary PDAC stromal and tumor signatures in the mouse stroma or human tumor cells. Lateral stacked bars correspond to the number of genes in each signature that is specifically expressed in PDX by mouse cells (green), human cells (red), or neither (gray).

(C) Tumor (red) and stromal (green) expression of genes in pathways known to be involved in tumor/stroma cross-talk. Values shown are median expressions, and error bars indicate first and third quartiles. References: I (Bergmann et al., 1995), II (Qian et al., 2003), III (Lonardo et al., 2011), IV (Ohnishi et al., 2003), V (Tian et al., 2009), VI (Whatcott et al., 2013), VII (Topalovski and Brekken, 2016), and VIII (Farrow et al., 2009).

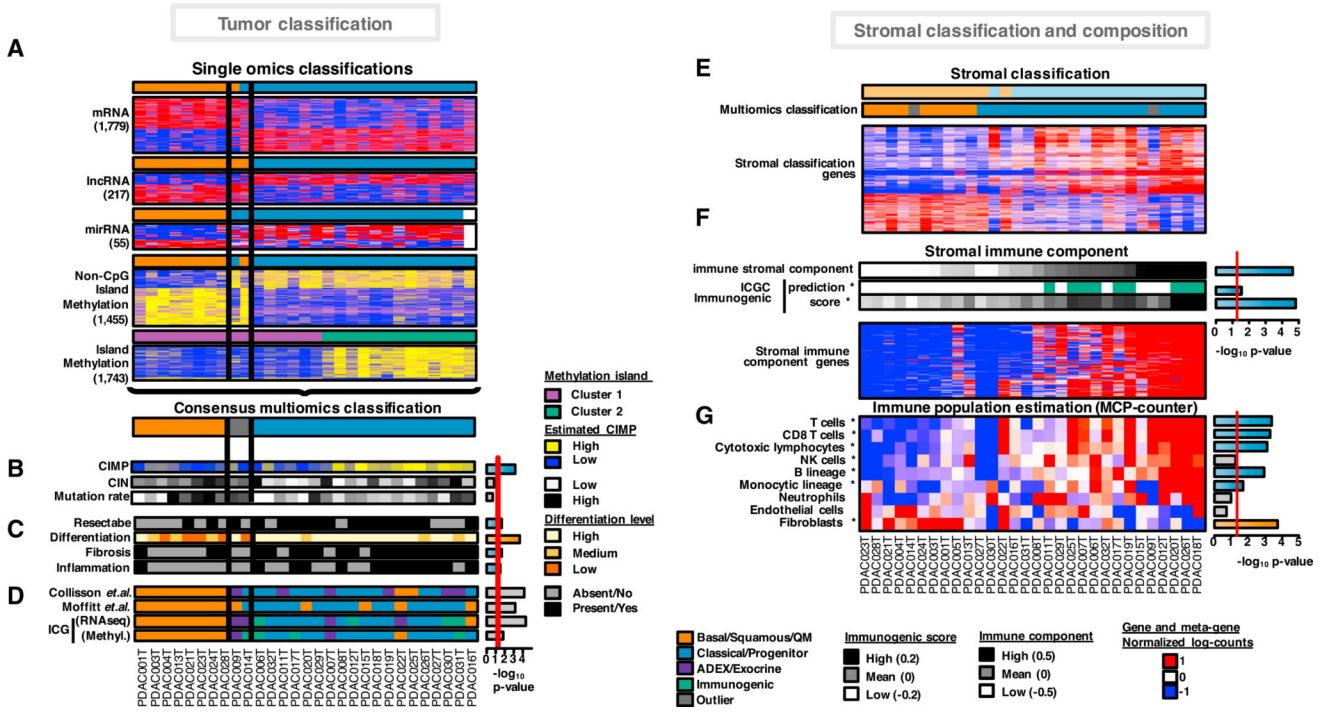

Figure 2. Tumor and Stroma Classifications

(A) Single-omics classifications and associated differential feature heatmaps used to define a consensus multiomics classification. Numbers in parentheses correspond to the number of differential features.

(B) Global epigenetic and genetic characteristics estimated from genome-wide assays. CIN, chromosomal instability index; CIMP, CpG island methylator phenotype.

(C) Clinical and histopathological characteristics.

(D) Primary human PDAC classification systems applied to the PDX tumor cell transcriptomes or methylation data (Methyl.). Lateral bars correspond to $-\log_{10}$ p value of Fisher's exact test of the association with the consensus multiomics classification (excluding outliers). Bars are colored when associated to a specific subtype (orange for basal; blue for classical) and significant ($p \leq 0.05$, indicated by red line).

(E) Consensus clustering applied to the stromal gene expression, generated from mouse RNA-seq reads. Heatmap represents expression values of all differentially expressed stromal genes between the two stromal subtypes.

(F) Immune stromal component sample projection and its contributing genes associated to the ICGC immunogenic subtype (prediction and score) applied to the stromal transcriptomes.

(G) Estimated level of infiltration of seven immune and two other stromal populations as computed by MCPcounter. Lateral bars correspond to $-\log_{10}$ p value of the association with the consensus multiomics classification (excluding outliers; Fisher's exact test or ANOVA). Bars are colored when associated to a specific subtype (orange for basal; blue for classical) and significant ($p \leq 0.05$). *$p \leq 0.05$, significant association with the stromal immune component (Pearson's correlation or ANOVA). All classifications and components analysis shown are based on unsupervised analysis of the associated datasets. Heatmaps show

Author Manuscript Author Manuscript Author Manuscript Author Manuscript

Author Manuscript Author Manuscript Author Manuscript Author Manuscript

expression/methylation values of the genes/CpG most associated with the unsupervised classification or component. All heatmaps are shown with the same samples in the same order.

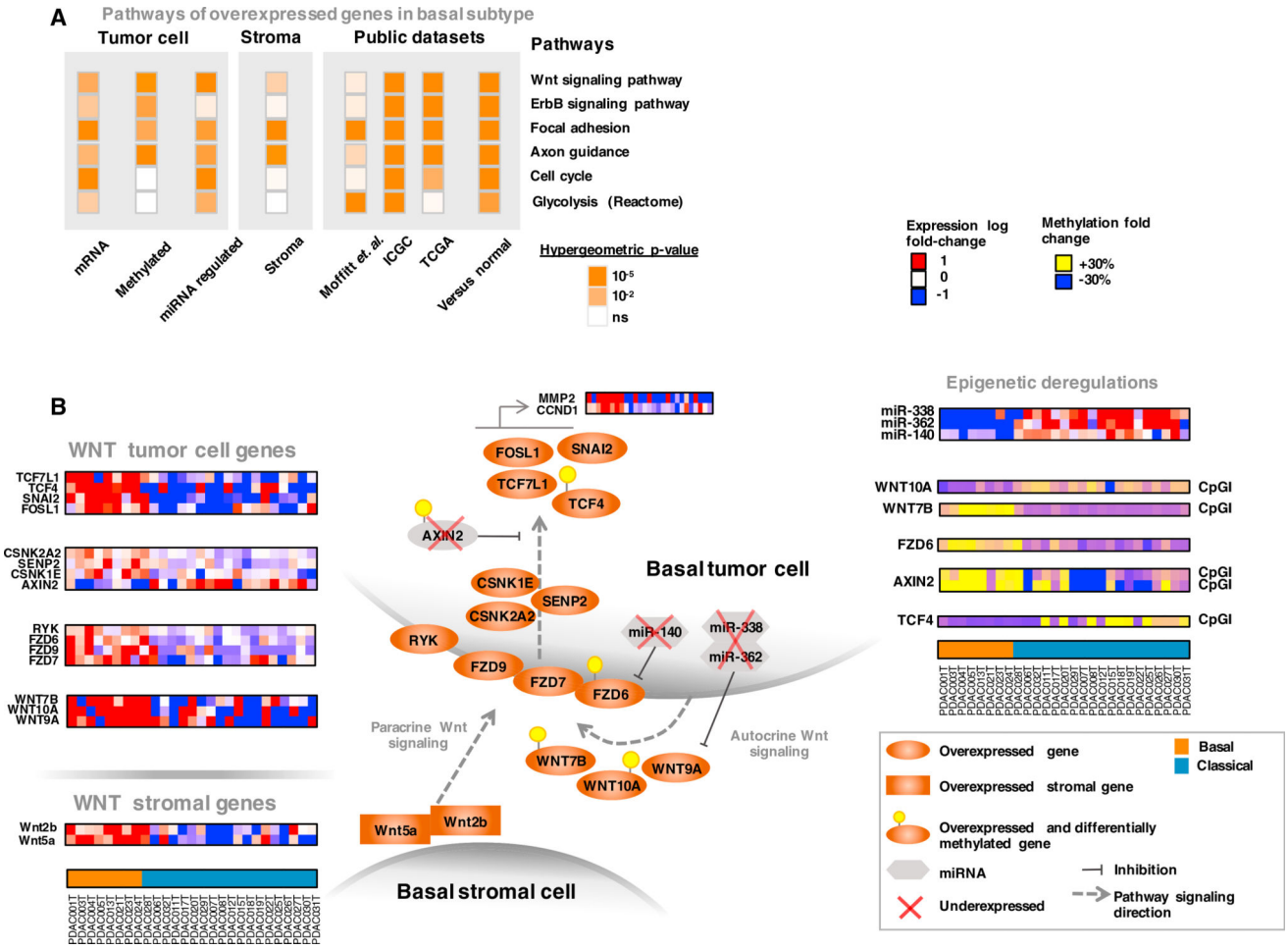

Figure 3. Basal Epigenetically Deregulated Pathways

(A) Basal pathway enrichment of: overexpressed genes (mRNA), overexpressed and differentially methylated genes (Methylated), overexpressed genes that are targets of underexpressed microRNA (miRNA regulated), genes overexpressed in the stroma of basal tumors (Stroma), overexpressed genes in the basal tumors of the Moffitt et al. (2015) dataset (Moffitt et al.), the ICGC dataset (ICGC), and the TCGA dataset (TCGA), and genes overexpressed in basal tumors compared to normal pancreatic samples (Versus normal). Pathway definition originates from the Kyoto Encyclopedia of Genes and Genomes (KEGG) database unless specified otherwise.

(B) Schematic illustration of the tumor and stromal deregulation of the WNT signaling pathway. Ellipses represent genes and hexagons miRNA found to be overexpressed (orange) or underexpressed (gray and crossed) in basal PDX tumors. Yellow circles indicate methylation-associated deregulation of expression. Rectangles represent genes overexpressed in basal PDX stroma. Blue-red heatmaps represent expression values of genes and miRNA. Blue-yellow heatmaps represent methylations values of CpG associated with genes. The CpGI annotation indicates that represented CpG methylation level originates from a CpG island. All heatmaps are shown with the same samples in the same order.

Author Manuscript Author Manuscript Author Manuscript Author Manuscript

Author Manuscript Author Manuscript Author Manuscript Author Manuscript

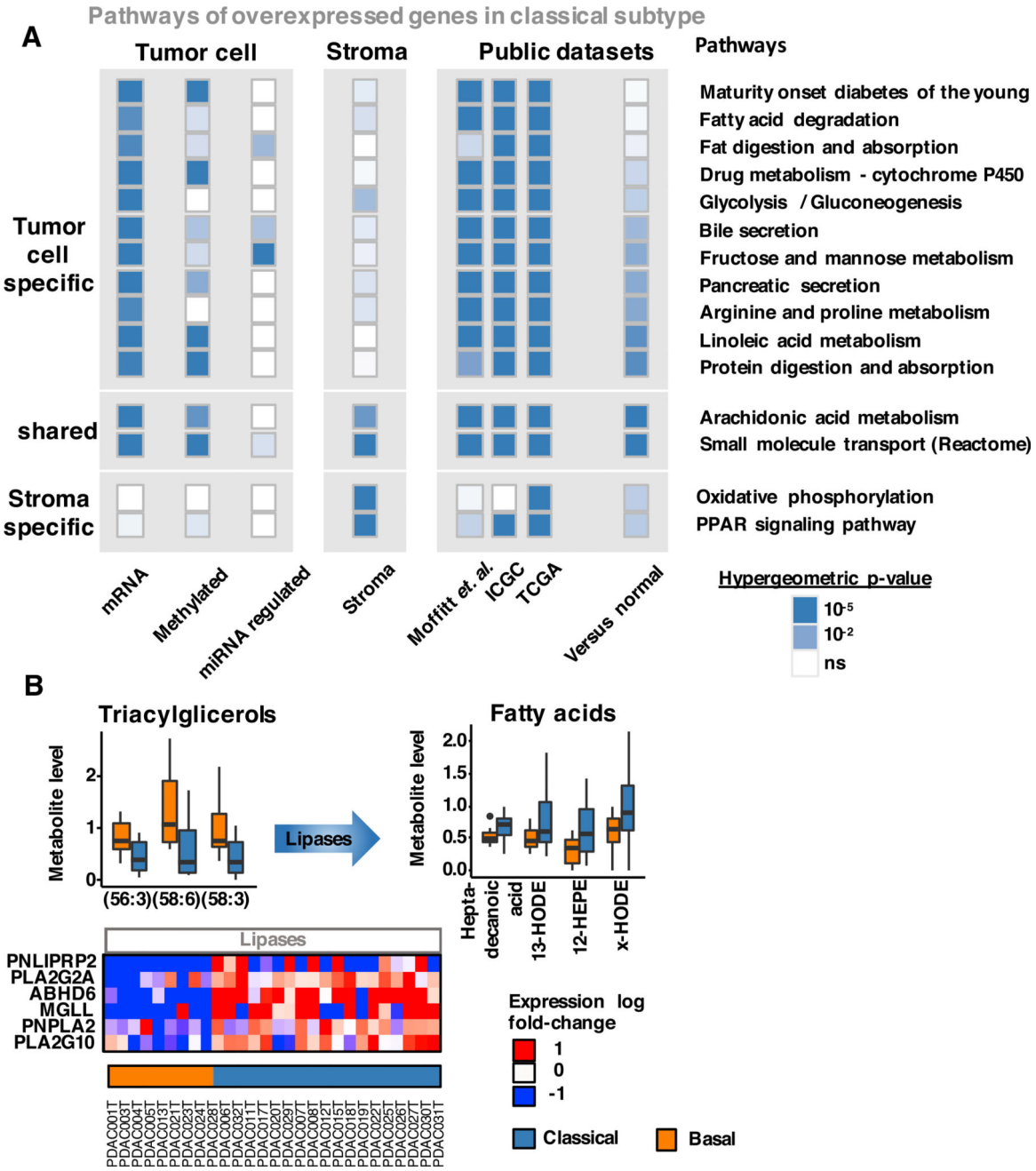

Figure 4. Classical Signaling and Metabolic Pathways

(A) Classical pathway enrichment of: overexpressed genes (mRNA), overexpressed and differentially methylated genes (Methylated) overexpressed genes that are targets of underexpressed micro-RNA (miRNA regulated), genes overexpressed in the stroma of classical tumors (Stroma), overexpressed genes in the classical tumors of the Moffitt et al. (2015) dataset (Moffitt et al.), the ICGC dataset (ICGC) and the TCGA dataset (TCGA), and genes overexpressed in Classical tumors compared to normal pancreatic samples (versus normal). Pathways are ordered by their tumor specificity compared to normal pancreatic

Author Manuscript Author Manuscript Author Manuscript Author Manuscript

samples and to the stroma. Pathway definition originates from the KEGG database, unless specified otherwise.

(B) Pancreatic lipase activity. Boxplots show the levels of the putative metabolic substrates (triacylglicerols, left) and products (fatty acids, right) of lipases in basal and classical samples. Expression of lipases is represented as a heatmap.

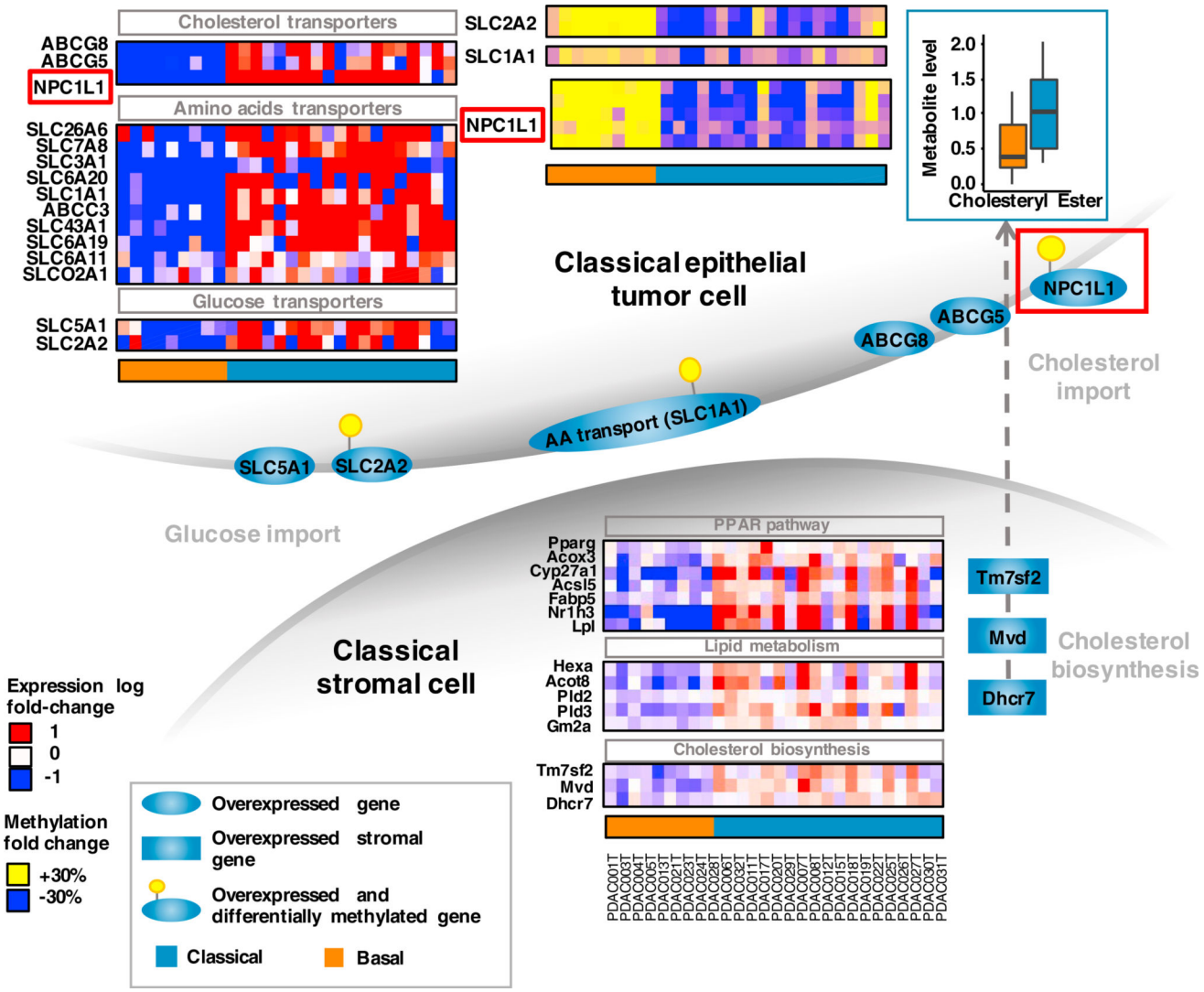

Figure 5. Classical Deregulated Tumor-Stroma Signaling Cross-Talk

Schematic illustration of the overexpressed transporters and stromal pathways in classical tumors. Ellipses represent genes overexpressed (blue) in classical PDX tumors. Yellow circles indicate methylation-associated deregulation of expression. Rectangles represent genes overexpressed in classical PDX stroma. Boxplots show the levels of cholesteryl ester in basal and classical samples. Blue-red heatmaps represent expression values of genes and miRNA. Blue-yellow heatmaps represent methylations values of CpG associated with genes. Arrows indicate the hypothetical flow of cholesterol. All heatmaps are shown with the same samples in the same order.

Author Manuscript Author Manuscript Author Manuscript Author Manuscript

Author Manuscript Author Manuscript Author Manuscript Author Manuscript

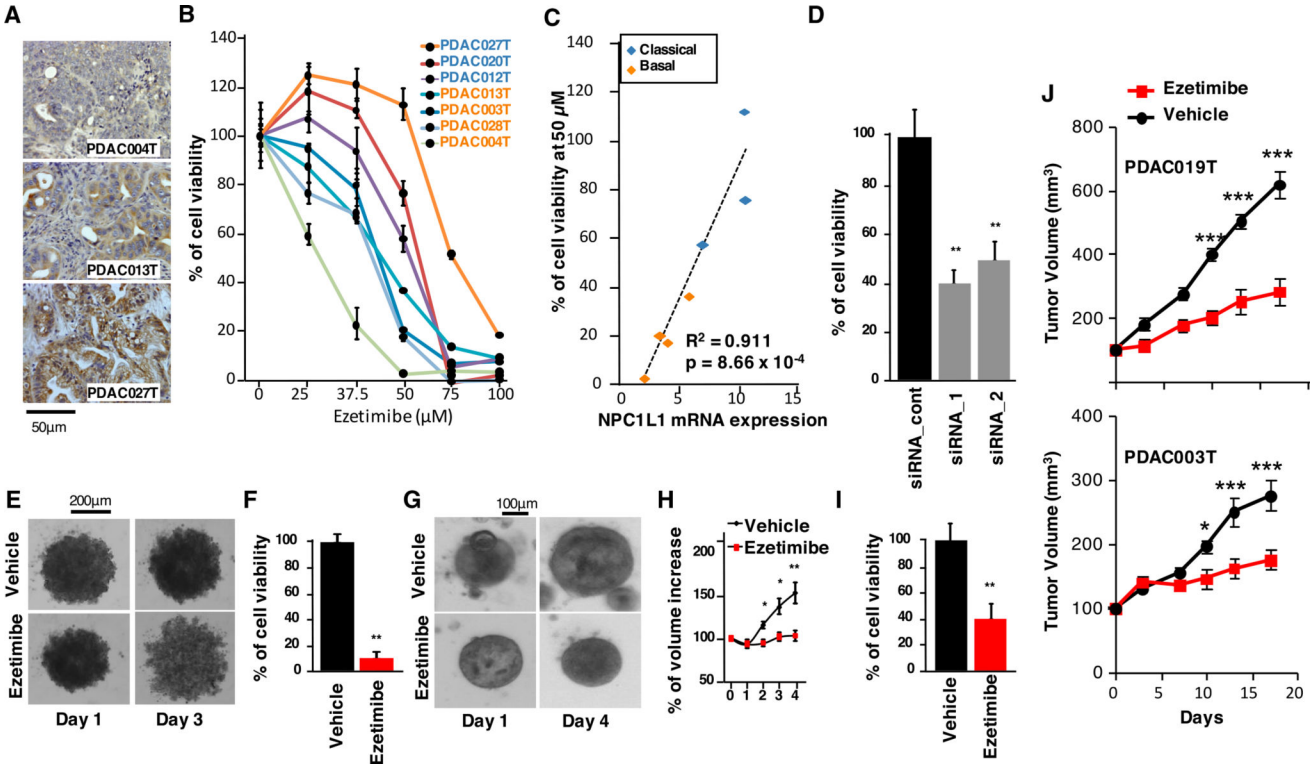

Figure 6. *NPC1L1* Is a Therapeutic Target for Treating PDAC

(A) Immunohistochemical staining of NPCL1L.

(B) Ezetimibe sensitivity of 7 PDX-derived cell lines. Dose-response curves after 72 hr of Ezetimibe treatment. The level of cell viability is represented as a percentage to the vehicle-treated control. Error bars represent SEM; n = 6.

(C) Correlation between survival percentage of Ezetimibe at 50 µM and *NPC1L1* mRNA expression for the 8 PDXs with Spearman correlation.

(D) Effect of knockdown *NPC1L1* with siRNA. si_RNA_1 and siRNA_2 directed against *NPC1L1* were transfected into PDAC012T, and survival was measured 72 hr later. Data are expressed as a percentage of siRNA_control (cont)-transfected cells.

(E and F) Effect of Ezetimibe on spheroid growth is indicated.

(E) Representative picture of the PDAC012T-derived spheroids treated with Ezetimibe (50 µM) or vehicle after 3 days.

(F) Cell viability of spheroids was measured by CellTiter Glo and expressed as percentage of the vehicle-treated spheroids. **$p < 0.01$.

(G–I) Effect of Ezetimibe on organoid growth is indicated.

(G) Representative picture of the PDAC012T-derived organoids treated with Ezetimibe (50 µM) or vehicle after 4 days.

(H) Calculated volume of organoids treated with Ezetimibe. *$p < 0.05$; **$p < 0.01$.

(I) Cell viability of organoids was measured by CellTiter Glo and expressed as percentage of the vehicle-treated organoids.

Author Manuscript Author Manuscript Author Manuscript Author Manuscript

(J) Two PDXs were treated with 5 mg/day of Ezetimibe or with vehicle for 17 days by i.p. injections (n = 3 per group). *$p < 0.05$; ***$p < 0.001$, in two-way ANOVA with Bonferroni post-test (mean ± SEM).